Impact of an Accidental Control Rod Withdrawal on the ALFRED core: Tridimensional Neutronic and Thermal-hydraulic analyses

M. Sarotto[1], G. Grasso[1], F. Lodi[2], G. Bandini[1], M. Sumini[2]

[1]Italian National Agency for New Technologies, Energy and Sustainable Economic Development (ENEA), Rome, Italy

[2]University of Bologna (UniBO), Bologna, Italy

E-mail contact of main author: massimo.sarotto@enea.it

Abstract. In the last years an international effort has been pursued for the development of the Advanced Lead Fast Reactor European Demonstrator (ALFRED) in line with the vision of the Gen-IV initiative for the LFR concept. This article - dealing with the ALFRED core design - analyses the global and local effects due to the accidental withdrawal of one control rod during the nominal plant state, by evaluating its impact in terms of reactivity balance and power distribution. Starting from the steady state neutronic results obtained with the ERANOS deterministic code, a detailed 3D power map of the core was evaluated (through a specific procedure) at the level of single fuel pins and used as input for accurate transient and thermal-hydraulic studies made by the RELAP5 system code and ANTEO+ sub-channel code, respectively. The ANTEO+ code, developed and validated by ENEA, was adopted to evaluate the temperature distributions in all the pins and surrounding sub-channels at key instants of the transient. It permitted the assessment of the new thermal conditions of the hot fuel assembly, in order to verify the compliance with the safety limits of the MOX fuel and the steel clad even in a completely unprotected scenario.

Key Words: ALFRED core, Accidental control rod withdrawal, Transient analyses, Sub-channel thermal-hydraulic analyses.

1. Introduction

In the last years an international effort has been pursued for the development of the Advanced Lead Fast Reactor European Demonstrator (ALFRED), whose design was initially conceived in the EURATOM FP7 LEADER project [1] and now is being carried on by the International Consortium FALCON (Fostering ALFRED Construction) signed by Italian, Romanian and Czech organizations [2]. In line with the vision of the Gen-IV initiative [3], the LFR concept following ALFRED is expected to excel in safety and economics while allowing the closure of the nuclear fuel cycle. After the LEADER project, the ALFRED design – and notably the design of the core [4] – has been refined along with a thorough investigation of the actual safety performances of the system, stressed against some extremely challenging conditions.

This article presents one of the punctual safety investigations performed to assess the ALFRED core design: the analysis of the global and local effects due to the accidental withdrawal, during nominal plant operation, of the Control Rod (CR) having the highest anti-reactivity worth. The impact on the core neutronics was evaluated in terms of reactivity balance and power distribution among Fuel Assemblies (FAs); furthermore, the distortion of the local power distribution in the hot FA was evaluated at the level of the single pin, in spite of the utilisation of a deterministic code. The steady state neutronic results were then used as input for accurate transient and Thermal-Hydraulic (TH) studies for the Unprotected Transient of Over-Power (UTOP) triggered by the CR withdrawal, in which the Temperature (T) distributions in all the pins and surrounding sub-channels of the hot FA were evaluated at

key instants of the transient. The main objective of the study was the assessment of the new thermal conditions of the hot FA in order to verify the compliance with the safety limits of both the fuel pellet and the clad even in a completely unprotected scenario.

This paper describes in some details: the ALFRED FA/core design and the local perturbation analysed (§2), the computational tools adopted (§3), the most significant results of the neutronic (§4), transient (§5) and sub-channel TH (§6) analyses. The concluding discussion points out at which extent the margins obtained for the fuel and clad should be high enough to accommodate the modelling, material properties and fabrication uncertainties, as well as the capability of the monitoring system to detect promptly the abnormal condition (§7).

2. ALFRED FA/core design and local perturbation analysed

The left part of *FIG. 1* depicts some details of the ALFRED fuel pin and FA design [1, 4]. The wrapped hexagonal FA encloses a triangular lattice of 127 positions, where 126 Mixed OXide (MOX) fuel pins surround the central dummy one. The pitch-over-diameter ratio in the lattice is quite large (1.32) in order to allow natural circulation in accidental conditions. The right part of *FIG. 1* shows a quarter of the core layout (having a 90° symmetry) that is essentially made of [1, 4]:

- 57 and 114 inner and outer FAs, respectively, having the same architecture but a different Pu enrichment (≅ 22% / 27% wt.% in inner / outer zone) for power distribution flattening;
- 4 Safety Rods (SRs) located in the centre of the core, which stay still atop the fissile zone during normal operation and enter the core for scram by gravity (ballast driven and pneumatically boosted);
- 12 CRs evenly positioned halfway in the outer fuel zone; the bank partly enters the active region from the bottom during operation to compensate the initial over-criticality and is progressively withdrawn as far as the refuelling condition is approached;
- the surrounding dummy assemblies, having the same structure of the FA but with pins filled by YZrO reflector pellets, thereby serving for both neutron economy and protection of the inner vessel.

The ALFRED fuel residence time is 5 years (at full-power irradiation) with a reloading scheme based on 5 batches without reshuffling of the FAs [1]: in the one-year irradiation sub-cycle, the reactivity is tuned by the 12 CRs. As shown in *FIG. 2*:

- at each Beginning of Cycle (BoC), the CRs are at their maximum operative insertion into the fissile zone; the anti-reactivity margin left (by the remaining part of the CR absorbing bundle which is withdrawn) can be exploited for scram (by buoyancy);
- at each End of Cycle (EoC), the CRs are completely withdrawn, so that the axial end stroke of their absorbing part is slightly below the fissile zone.

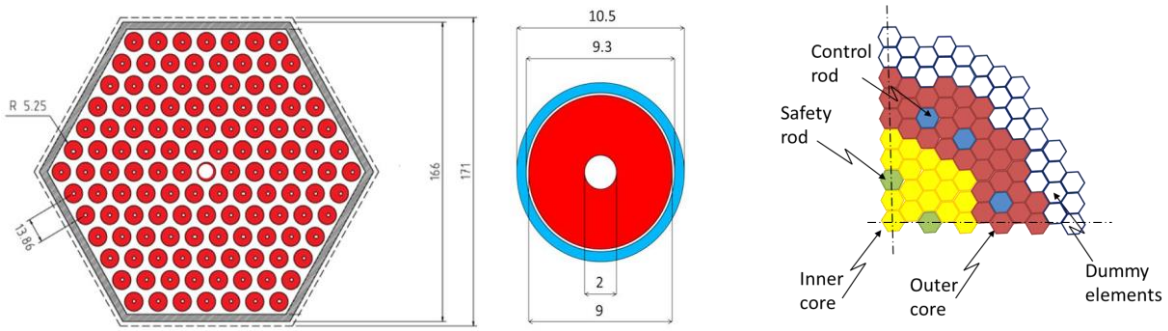

FIG. 1. ALFRED FA and fuel pin design (left frame); ALFRED core layout (right frame).

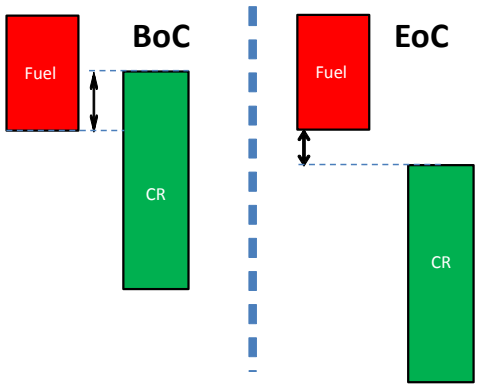

FIG. 2. Axial position of the CR absorbing bundle relative to the fissile core (not in scale) at BoC (left frame) and EoC (right frame).

The impact of the CR accidentally withdrawn – in terms of reactivity effect and distortion of the power distribution – was conservatively evaluated at BoC, that is the moment during operation when the 12 CRs are actually inserted the most into the fissile zone. The CR is withdrawn down to the end stroke (EoC configuration in *FIG. 2*), while the other (11) CRs are maintained in the BoC position. For easiness, the impact of such event on the core neutronics was evaluated with fresh fuel compositions in the whole core: this assumption results anyway conservative, being the importance of outer FAs the highest with fresh fuel.

3. Computational tools

The neutronic analyses were carried out with the ERANOS ver. 2.2 deterministic code [5] coupled with the JEFF3.1 nuclear data library [6]. The cross-sections of the different core regions were produced by a 1968 energy-groups analysis and condensed to the standard structure at 33 groups by the ECCO cell code [7]. The macroscopic cross-sections were then used for full core calculations carried out with the TGV module [8], by adopting the variational nodal method in a 3D hexagonal (hex-Z) geometry model of the core.

By exploiting the ECCO power distribution obtained through a 2D heterogeneous model of the FA[1] and by super-imposing on it the shape of the core flux in the position of the hottest FA (interpolating the nodal flux on the pins locations by means of a dedicated routine), the power distribution inside the FAs of interest was accurately evaluated at the level of single pins. The core "global" and FA "local" power distributions are here shown also in a graphical form through an in-house python script.

Besides changing the power deposition among the FAs, the spurious withdrawal of a single CR is also assumed to initiate an UTOP transient due to the associated insertion of positive reactivity. For evaluating the transient behaviour stemming from the inserted reactivity, the RELAP5 system code was adopted [9]. The TH analyses were then carried out with the sub-channel code ANTEO+ [10], developed in-house at ENEA specifically for liquid metal (*e.g.*, Na, Pb and Pb-Bi) cooled systems and extended to encompass any (possibly conceived) advanced FA design, as in some of the reactor concepts envisaged within the GIF initiative. The ANTEO+ model of the ALFRED FA is depicted in the left part of *FIG. 3* along with the conventional pin numbering, while the right part of the same figure defines the three kinds of sub-channel (interior, edge and corner) for these bundle geometries. As for the neutronic analyses, the ANTEO+ results are here shown graphically through a dedicated python routine.

[1] The ECCO geometry model describes the horizontal section of the FA at the level of pins (and wrapper, see left frame of *FIG. 1*), while axial leakages are taken into account by tuning the buckling value [7].

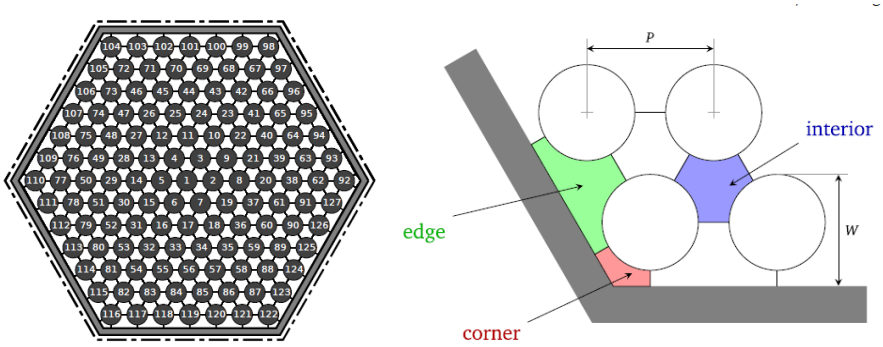

FIG. 3. FA model in ANTEO+ with pin numbering (left frame); three types of sub-channel in a hexagonal assembly (triangular pin lattice, right frame).

As described in [10], the modelling adopted in ANTEO+ corresponds to a system of sub-channels dynamically connected only at the inlet and energetically connected throughout the whole simulated (axial) development of the bundle. Once the coolant T distribution is known, the internal T distribution of the fuel pin can be calculated consequently. Since ANTEO+ does not integrate any advanced thermo-mechanic module, the maximum fuel and clad Ts are estimated approximatively (*e.g.*, un-irradiated conditions, cold geometry, clad-fuel gap filled with helium); nonetheless this approximation is deemed acceptable for the present purposes.

4. Neutronic analyses in steady state conditions

Starting from the BoC nominal state, the variation of the effective multiplication factor (k_{eff}) was evaluated in the perturbed core conditions (§2). With the complete withdrawal of one CR, the corresponding Δk_{eff} - expressed in per cent mille (pcm) - results +222 pcm, that is safely lower than the delayed neutron fraction (≅340 pcm), as designed. To be noticed that, for the symmetry of the core layout (right part of *FIG. 1*), each CR yields almost the same (anti-) reactivity worth.

FIG. 4 reports the radial core power distributions at BoC in nominal and perturbed conditions: the "ff_rad" values indicate the power distribution factors (ratios local-to-average) of every FA in a red-green-blue (rgb) scale. It results evident that the hot FA belongs to the inner fuel zone in nominal conditions and to the outer one (close to the withdrawn CR) in the perturbed state.

Table I reports the values at BoC (in both nominal and perturbed conditions) and at EoC of the radial, axial and total power peaking factors: namely "ff_{rad_core}", "ff_{rad_HotFA}", "ff_{ax_HotFA}" and "ff_{tot_core}" (*i.e.*, $ff_{tot\_core} = ff_{rad\_core} \times ff_{rad\_HotFA} \times ff_{ax\_HotFA}$). The radial power distribution among the FAs was evaluated in the inner and outer zones separately: trivially, the highest values indicated by bold characters represent the "ff_{rad_core}" peaking factor (and correspond to the maximum ff_rad values reported in *FIG. 4*). The radial distribution among the pins in the hot FA (ff_{rad_HotFA}) was also evaluated in the inner and outer zones separately, as well as the axial peaking factors in the hot FA (ff_{ax_HotFA}). It can be noticed that the highest value of the total peaking factor (ff_{tot_core}) occurs at the BoC perturbed state in the hot FA of the outer zone, close to the CR completely withdrawn.

Finally, *FIGS. 5* and *6* show the pin power distributions through the values of the radial peaking factors "ff_rad" for each pin in the hottest FAs in the inner and outer zones. The distributions refer to the nominal (*FIG. 5*) and perturbed (*FIG. 6*) BoC core conditions. They were used as input for the ANTEO+ TH analyses in the nominal BoC (and EoC) states; differently, for the perturbed case, the transient analyses resulted necessary (§5).

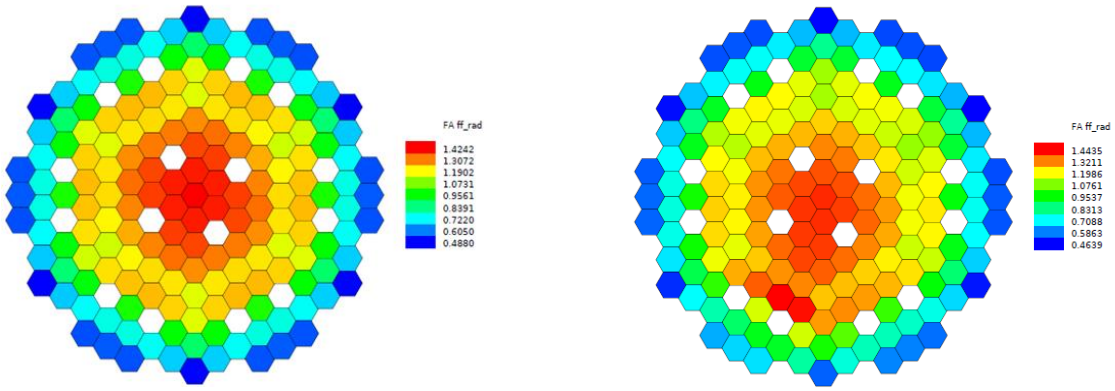

FIG. 4. Core power distributions in the BoC nominal (left frame) and perturbed (right frame) states.

TABLE I: Radial, axial and total power peaking factors in the inner zone, outer zone and in the whole core for the BoC (nominal and perturbed) and EoC (nominal) core states.

Core	**ff_{rad_core}**			**ff_{rad_HotFA}**		**ff_{ax_HotFA}**		**ff_{tot_core}**	
Condition	**Inner**	**Outer**	**Core**	**Inner**	**Outer**	**Inner**	**Outer**	**Inner**	**Outer**
BoC nominal	**1.424**	1.252	1.424	**1.0236**	1.0962	**1.149**	1.220	**1.675**	1.674
BoC perturbed	1.405	**1.444**	1.444	1.0251	**1.0628**	1.149	**1.182**	1.655	**1.814**
EoC	1.188	**1.270**	1.270	1.0227	**1.0535**	1.142	**1.168**	1.387	**1.563**

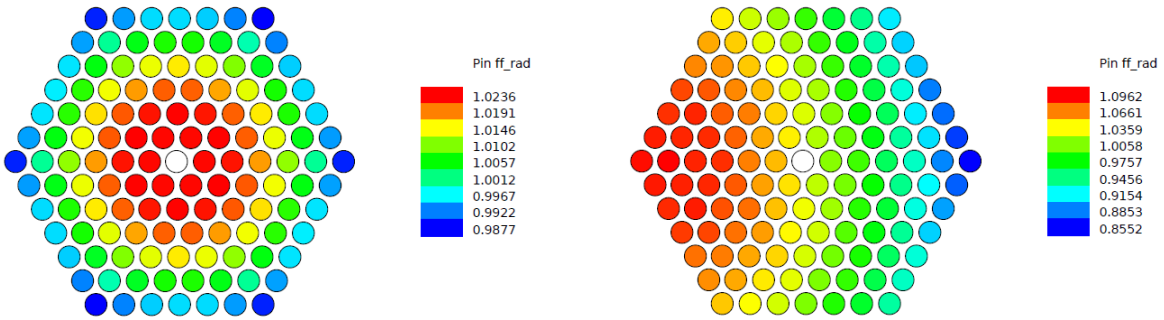

FIG. 5. Radial peaking factors for each pin of the hot FA in the inner zone (left frame) and outer zone (right frame) in the BoC nominal state.

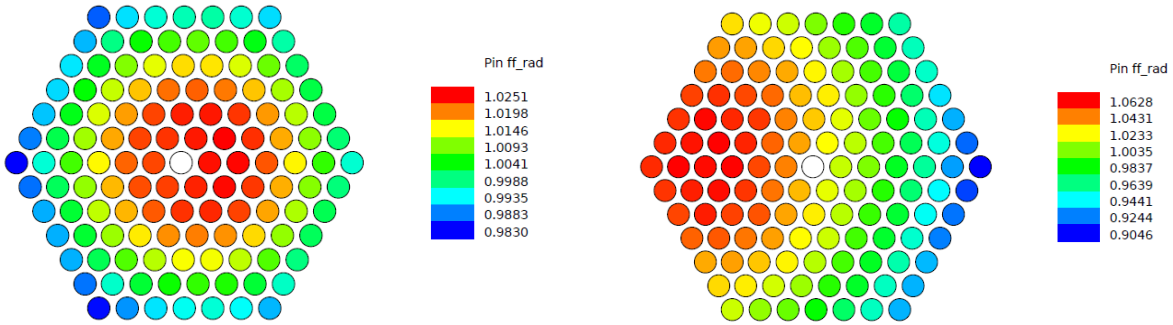

FIG. 6. Radial peaking factors for each pin of the hot FA in the inner zone (left frame) and outer zone (right frame) in the BoC perturbed state.

5. Transient analyses

The spurious withdrawal of a single CR initiates a TOP transient due to the associated insertion of positive reactivity. In order to evaluate the thermal performances of the fuel, the maximum power reached in such transient - supposed unprotected to be conservative - was established. Thus the first step was to select the credible maximum withdrawal velocity of the CR which is fixed by the maximum actuation speed of the motor moving the CR handler[2]. The adopted choice was based on the European Utility Requirements for modern nuclear power plants [11], which states that a power variation of around 5% per minute should be a design target. Given the 300 MW_{th} power of the ALFRED reactor, this translates in 0.25 MW_{th} s^{-1} and considering that in [12] the extraction of some 3 mm of the 12 CRs gives a power rise of about 18 MW_{th} (corresponding to 0.5 MW_{th} mm^{-1} for the single CR), the necessary extraction velocity results of 0.5 mm s^{-1}. Coupling the extraction velocity with the CR reactivity curve (giving the worth of the CR for each axial position) reported in [12] and normalizing to the total worth of the CR extracted (§4), the relation between time and the inserted reactivity can be finally obtained. The net result is depicted in *FIG. 7* and represents the input for the transient analysis.

For evaluating the transient behaviour with the RELAP5 system code, modified by ENEA and Ansaldo Nucleare for LFR applications, the reactivity coefficients reported in Table II were used and the results obtained are depicted in *FIG. 8*. The maximum core power in the transient occurs at about 450 s and sets at 464 MW_{th} (~1.55 times the original power, see left part of *FIG. 8*) to which corresponds a core inlet T of 445.5 °C (see right part of *FIG. 8*). To better understand the transient dynamics, the left part of *FIG. 9* shows that the inserted reactivity from the withdrawn CR is almost counterbalanced by: the fuel Doppler effect, the radial core expansion (due to the increasing core inlet and outlet Ts), the axial fuel expansion, the coolant and CR driveline thermal expansions. The net reactivity stays slightly positive as long as the CR withdrawal takes place thus driving the power increase; once the withdrawal is completed (at about 450 s), the reactivity becomes negative and the point of maximum power is reached. Then, the various effects balance each other bringing the core toward a new steady state power, as depicted in the right part of *FIG. 9*.

For understanding the evolution of the inlet T (shown in the right part of *FIG. 8*), it must be reminded that the primary circuit mass flow is basically constant during the transient, implying that a core power increase translates in a higher core outlet T. Due to the steam generators and balance of plant capability, during the transient phase of the UTOP the core power exceeds the power removed by the secondary system, thereby leading the steam generator outlet T (that is also the core inlet T) to increase until the two systems converge to the new steady state power, as visible in the right part of *FIG. 9*.

TABLE II: Main reactivity coefficients at nominal BoC and EoC core states [1].

Core Condition	Doppler constant (pcm)	Axial fuel expansion (pcm K^{-1})	Coolant expansion (pcm K^{-1})	Axial clad expansion (pcm K^{-1})	Radial core expansion (pcm K^{-1})	CR drive expansion (pcm mm^{-1})
BoC	-555	-0.148	-0.271	0.037	-0.762	-19.2
EoC	-566	-0.155	-0.268	0.039	-0.789	-9.3

[2] This velocity should be as low as possible to reduce the effect of a sudden CR extraction in an UTOP and, at the same time, as high as possible to allow a fast regulation increasing the reactor load following capabilities.

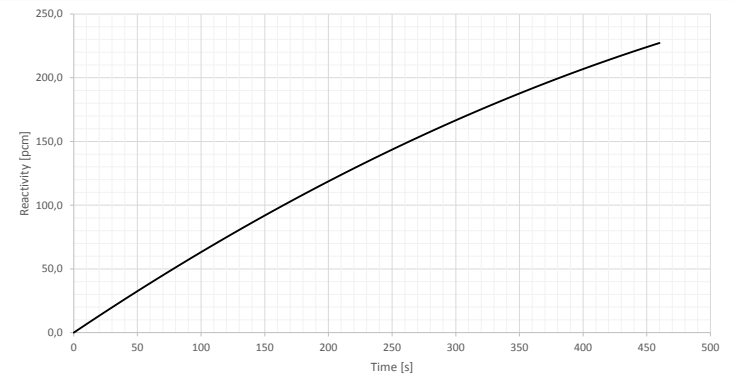

FIG. 7. Reactivity insertion as a function of time for the UTOP.

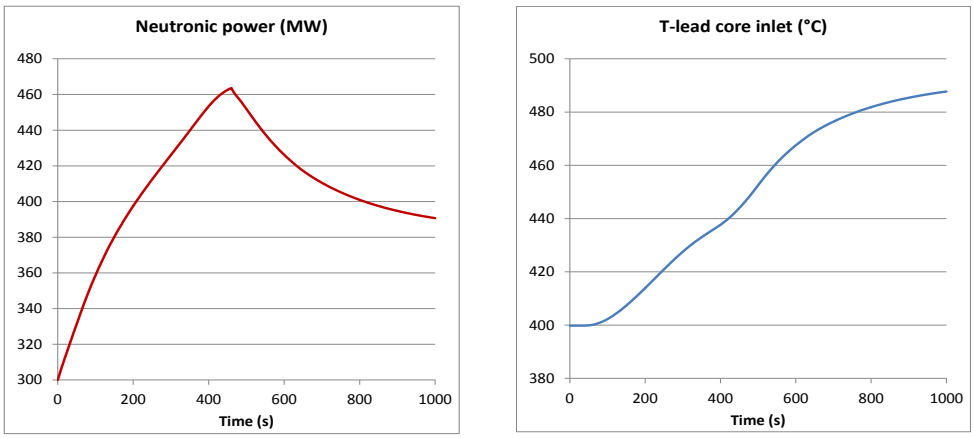

FIG. 8. Core power (left frame) and coolant inlet T (right frame) as a function of time during the UTOP.

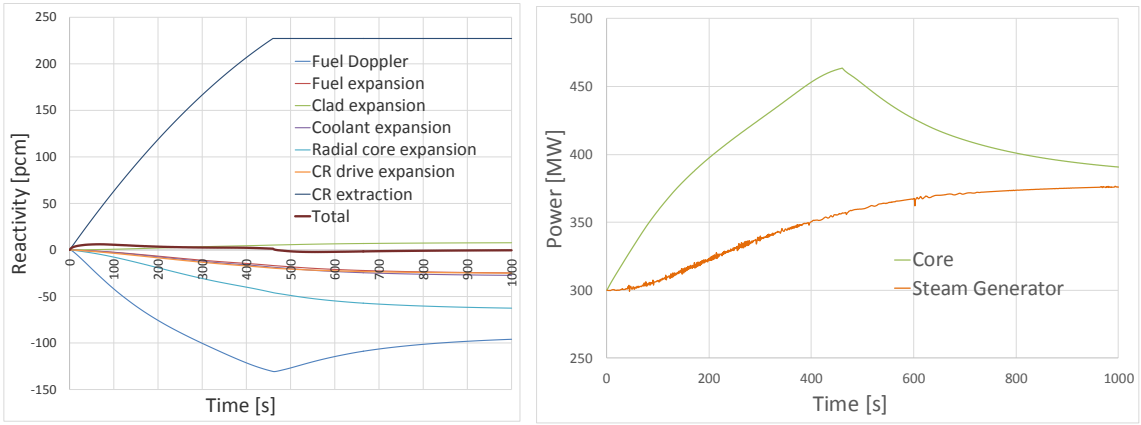

FIG. 9. Various feedback contributions to the total reactivity during the UTOP (left frame); core and steam generator power evolution during the UTOP (right frame).

6. Sub-channel TH analyses

Starting from the neutronic results in steady states (§4), *FIG. 10* shows the distribution of the coolant outlet T in the hot FAs of the inner and outer zones at nominal BoC state, as obtained by the ANTEO+ code. As expected, the T distribution is more uniform in the hot FA of the inner zone (away from CRs). The hot sub-channels are the corner ones in both inner and outer zones: the hottest one appears in the inner FA with an outlet T of ≅ 492 °C.

The core behaviour during the transient was calculated updating the FA power distribution in the perturbed state (*FIG. 6)* with the new overall core power during the UTOP (left part of *FIG. 8*) and using the new core inlet T at the point of maximum power (right part of *FIG. 8*). This methodology enabled the correct evaluation of the safety performances of the core. The hottest sub-channels appear in the hot outer FA and the corresponding radial T distribution is reported in *FIG. 11*: the maximum outlet T reaches ≅ 615 °C.

Finally, *FIG. 12* plots the axial distribution of the maximum clad and fuel Ts (in the hot pin of the hot FA in outer zone) in the point of maximum power during the transient, compared with the ones in the BoC nominal state. As can be seen from the right part of *FIG. 12*, the maximum fuel T results of 2544 °C (at a local linear power of 577 W cm^{-1}). Given the conservative estimation (*i.e.*, ANTEO+ evaluates the fuel T with correct material properties but cold geometry), with respect to the melting T of ≅ 2700 °C [13] the margin should be high enough to accommodate the modelling, operative (including measurement), material properties and fabrication uncertainties. Fuel melting should then be excluded even in case the TOP initiated by the spurious withdrawal of one CR actually evolved as unprotected (*i.e.*, none of the safety systems acted to stop the transient). Therefore, the focus on the long term would be on the clad (and its ability to withstand creep), whose peak T (*i.e.*, hottest pin in the hottest FA) reaches ≅ 670 °C (see left part of *FIG. 12*).

At the peak clad T of 670 °C (evaluated at half-thickness), the time-to-rupture is in the order of some weeks, even to sustain the inner pressure of a completely burnt FA. This fact well meets the recommendations of the safety regulators, which set in 30 minutes into the accident the time for which any operators' intervention cannot be credited. Therefore, the huge grace time for intervention allowed by the clad time-to-rupture makes highly probable that the unprotected condition is arrested by actuation of a backup scram and, consequently, no cladding failure can be expected should this kind of accident occur.

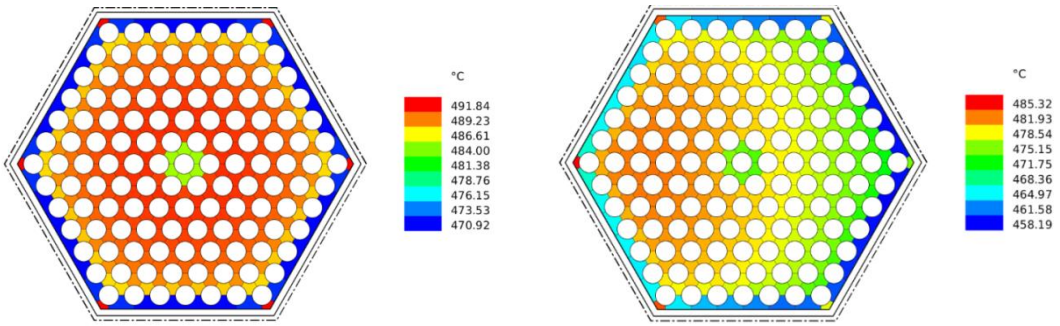

FIG. 10. Radial distribution of the coolant outlet T in the hot FAs in the inner zone (left frame) and outer zone (right frame) in the BoC nominal state.

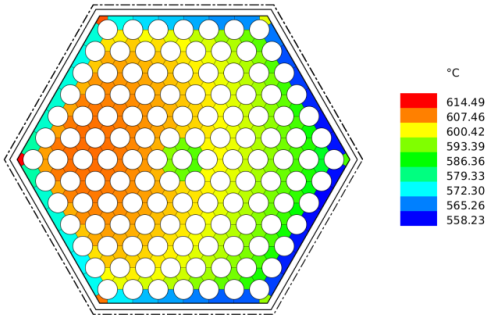

FIG. 11. Radial distribution of the coolant outlet T in the hot FA (in the outer zone close to the CR accidentally withdrawn) in the point of maximum core power during the UTOP.

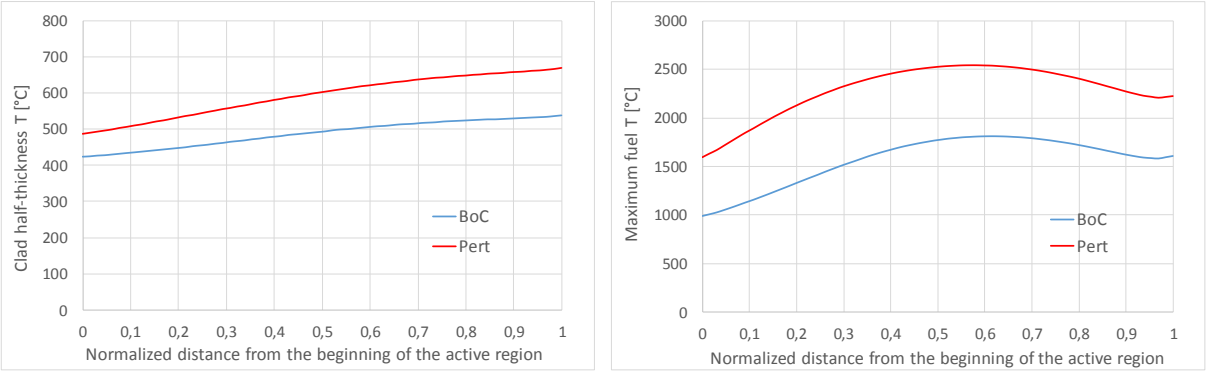

FIG. 12. Axial distribution of the maximum clad (left frame) and fuel pellet (right frame) temperatures in the point of maximum core power for the UTOP (Pert) along with the same profile at nominal BoC.

7. Concluding discussion

The global and local effects due to the spurious withdrawal of the CR having the highest anti-reactivity worth were evaluated, assuming such a scenario as one of the most challenging perturbations potentially occurring during the nominal plant conditions of the ALFRED reactor, aiming to be the European demonstrator for the LFR. The main objective of the study was the assessment of the new thermal conditions of the hottest FA in order to verify the compliance with the safety limits even in the perturbed condition or, alternatively, the capability of the monitoring system to detect promptly the abnormal condition.

These effects were evaluated by means of neutronic, transient and TH analyses carried out by means of the ERANOS deterministic code, the RELAP5 system code and the ANTEO+ (ENEA's in-house tool) sub-channel code, respectively. The neutronic analyses provided the core reactivity balance (+220 pcm reactivity), as well as the global power distribution among the FAs and the local one in the hot FA at the level of single pins. The neutronic results were used as input for the study of the TOP transient initiated by the spurious withdrawal of the CR. For conservativeness, the transient was also assumed to evolve in unprotected conditions. By adopting a credible maximum withdrawal speed [11], the transient analysis provided a maximum core power in the simulated UTOP of 464 MW_{th} (~1.55 times the nominal power) at about 450 s, with a corresponding core inlet T of about 445 °C.

Successively, an accurate TH study was carried out to evaluate the T distributions in all the pins and surrounding sub-channels of the hot FA. In the transient between the nominal BoC state and the UTOP conditions, in the hot pin the peak clad T increases from 525 °C up to 670 °C and the peak fuel T increases from 1930 °C up to 2544 °C. Since the conservative evaluation, a margin remains in the UTOP case against fuel melting, which is deemed sufficient to accommodate the modelling, operative (including measurement), material properties and fabrication uncertainties. Therefore, fuel melting could be excluded even if none of the safety systems acted to prevent, or early stop, the UTOP. Similarly, by looking at the clad T behaviour and its ability to withstand creep, the resulting grace time for operators' intervention (some weeks) is high enough to exclude clad failures, even by considering the highest inner pressure in a FA at the end of life and the extra release of fission gases due to the UTOP itself.

It is worth however mentioning that, even if the safety requirements are met without any operators' intervention, clear signals should be detected by the reactor protection system:

- the power (and thus flux) increases by almost 55%, that should be detected by the operation neutron detectors as described in [14];

- the coolant outlet T increases (notably, for the hot FA, the average T raises from 475 °C in nominal conditions up to 594 °C in the UTOP ones), so that the thermocouples at the outlet nozzle of each FA should be able to detect such a significant shift.

Therefore, if any of these signals succeeds in activating a scram, the transient just described would be promptly cut, the unprotected condition being turned into a protected state, thereby extending indefinitely the grace time with no safety implications at all.

Acknowledgements

The computing resources and the related technical support used were provided by the CRESCO/ENEAGRID High Performance Computing infrastructure and its staff (www.cresco.enea.it), funded by ENEA and by national and European research programs.

References

[1] GRASSO, G., *et al.*, "The core design of ALFRED, a demonstrator for the European lead-cooled reactors", Nucl. Eng. and Des., Vol. **278** (2014), 287-301.

[2] International Consortium FALCON (Fostering ALfred CONstruction) (2013), https://www.euronuclear.org/e-news/e-news-43/ansaldo.htm.

[3] OECD/NEA. Technology Roadmap Update for Generation IV Nuclear Energy Systems (2014), .

[4] LODI, F., *et al.*, "Characterization of the new ALFRED core configuration", ENEA Tech. Rep. ADPFISS-LP2-085 (2015).

[5] RIMPAULT, G., *et al*., "The ERANOS code and data system for Fast Reactor neutronic analyses", Proc. Int. Conf. *New frontiers of Nuclear Technology: reactor physics, safety and high-performance computing*, PHYSOR 2002, Seoul, Korea, October 7-10th (2002).

[6] KONING, A., *et al.*, "The JEFF-3.1 Nuclear Data Library", NEA Data Bank, OECD, JEFF Report 21, NEA N_6190 (2006).

[7] RIMPAULT, G., "Physics documentation of Eranos: the Ecco cell code", CEA Tech. Rep. DERSPRC-LEPh-97-001 (1997).

[8] RUGGERI, J.M., *et al.*, "TGV: a coarse mesh 3 dimensional diffusion-transport module for the ERANOS code system", CEA Tech. Rep. DRNR-SPCILEPh-93-209 (1993).

[9] FLETCHER, C.D., *et al.*, "RELAP5/MODE3 code manual", NUREG/CR–5535, INEL–95/174, Idaho National Engineering Laboratory (1995).

[10] LODI, F., *et al.*, "ANTEO+: a sub-channel code for thermal-hydraulic analysis of liquid metal cooled systems", Nucl. Eng. and Des., Vol. **301** (2016), 128-152.

[11] LOKHOV, A., "Technical and economical aspects of load following with nuclear power plants", NEA Nuclear Development Division, OECD-NEA (2011).

[12] PONCIROLI, R., *et al.*, "Object-oriented modelling and simulation for the ALFRED dynamics", Progress in Nuclear Energy, Vol. **71** (2014), 15-29.

[13] POPOV, S.G., *et al.*, "Thermophysical properties of MOX and UO2 fuels including the effects of irradiation", ORNL Tech. Rep. ORNL/TM-2000/351 (2000).

[14] GUGLIELMELLI, A., *et al.*, "Studi preliminari di tecniche di monitoraggio del nocciolo di ALFRED", ENEA Tech. Rep. ADPFISS-LP2-051 (2014).